Calhoun: The NPS Institutional Archive

DSpace Repository

Theses and Dissertations | 1. Thesis and Dissertation Collection, all items

1955

Experiments on improving the efficiency of the Bevatron Ion Source.

Stone, Troy Edward

Monterey, California: U.S. Naval Postgraduate School

Downloaded from NPS Archive: Calhoun

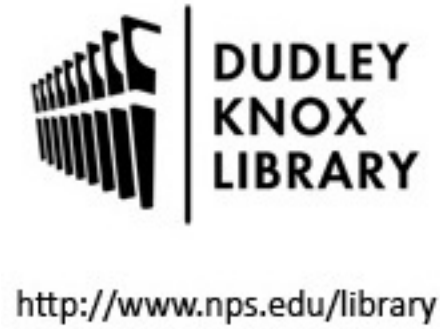

http://www.nps.edu/library

Calhoun is the Naval Postgraduate School's public access digital repository for research materials and institutional publications created by the NPS community. Calhoun is named for Professor of Mathematics Guy K. Calhoun, NPS's first appointed -- and published -- scholarly author.

Dudley Knox Library / Naval Postgraduate School
411 Dyer Road / 1 University Circle
Monterey, California USA 93943

EXPERIMENTS ON IMPROVING THE EFFICIENCY OF THE BEVATRON ION SOURCE

TROY EDWARD STONE

Library
U. S. Naval Postgraduate School
Monterey, California

DUDLEY KNOX LIBRARY
NAVAL POSTGRADUATE SCHOOL
MONTEREY, CALIFORNIA 93943-5002

EXPERIMENTS ON IMPROVING THE EFFICIENCY OF THE BEVATRON ION SOURCE

by

Troy Edward Stone

Lieutenant, United States Navy

Submitted in partial fulfillment
of the requirements
for the degree of
MASTER OF SCIENCE
IN
PHYSICS

United States Naval Postgraduate School
Monterey, California

1955

5765

This work is accepted as fulfilling

the thesis requirements for the degree of

MASTER OF SCIENCE

IN

PHYSICS

from the

United States Naval Postgraduate School

Library
U. S. Naval Postgraduate School
Monterey, California

ABSTRACT

A study has been conducted to determine the focal properties of an ion source that is typical of those used with the Bevatron. Beam-intensity patterns have been obtained for various focusing conditions. The effects of space-charge repulsion and lens aberration have been investigated. Losses through Coulomb scattering on residual gas molecules have been observed, and a curve showing variation of these losses with variation of energy through the focus electrode has been obtained. Pressure throughout the accelerating column was found to be an important factor, and losses occasioned through slight increases in the normal operating pressure have been recorded.

All previous ion sources for the Bevatron have been designed for presentation of a real image to the subsequent injection system. A virtual-image source has been designed, constructed and tested on the Bevatron.

ABSTRACT

A study has been conducted to determine the focal properties of an ion source that is typical of those used with the Electron Beam-Ion Metering Rate Beam deposition for etching conditions. The effects of space-charge repulsion and time-of-flight have been investigated. Lenses through Gaussian matching or reversed gas molecules have been observed, and a cubic shooting solution of the Lenses with weighted of energy through the focal electron-ion beam focused. Precision through the accelerating column has found to be an important factor, and limits associated through slight increases in the normal operating pressure have been reduced

All previous ion sources for the Electron have been designed to prevent of a real image to the subsequent lenses. A virtual-image source has been designed, constructed and tested on the Electron

PREFACE

A continuing and intensive effort is being made to increase the magnitude of the output beam of the Bevatron. Refinements in the machine itself during the past year have resulted in a current intensity approaching 10^{10} protons per pulse, a most significant improvement; but considerably better performance than this is envisioned. Increasing the output and (or) improving the efficiency of the Bevatron' ion source is one way of attaining more beam, and to this end work has been conducted during the past year by the writer.

This experimentation was conducted under the guidance of Dr. B. B. Kinsey, formerly of the Chalk River Atomic Energy Project and during the past year a visiting scientist at the University of California Radiation Laboratory. Frequent recourse has been made to the knowledge and experience of Bruce Cork of the Bevatron staff. The writer is particularly indebted to them for their enlightenment, assistance, and encouragement during the course of this work.

The writer wishes to thank Professor N. L. Oleson of the U. S. Naval Postgraduate School for his assistance in the preparation of this paper.

This work was conducted under the auspices of the U. S. Atomic Energy Commission while the writer was attached to the University of California Radiation Laboratory.

TABLE OF CONTENTS

Item	Title	Page
Abstract	. . . . .	ii
Preface	. . . . .	iii
List of Illustrations	. . . . .	v
Chapter I	Introduction	1
Chapter II	Focal Properties of a Typical Ion Source . .	5
Chapter III	Losses through Space-Charge Repulsion, Lens Aberration, Coulomb Scattering, and Residual Gas	10
Chapter IV	Design and Test of a Virtual-Image Ion Source	16
Bibliography	. . . . .	20

TABLE OF CONTENTS

Item	Title	Page
Abstract		i
Preface		iii
List of Illustrations		v
Chapter I	Introduction	1
Chapter II	Basic Principles of a Thermal Ice Sensor	3
Chapter III	Sensor Design Through Analog Computation: Heat Conduction, Phase Change, Convection, Radiation, and Electronic Effects	10
Chapter IV	Design and Test of a Working Prototype Ice Sensor	45
Bibliography		69

LIST OF ILLUSTRACTIONS

Figure		Page
1.	Block Diagram of Ion Source	21
2.	Cross Section of Arc Chamber	22
3.	Focusing Action of Three Electrodes	23
4.	Block Diagram of Bevatron Injection System	24
5.	Original Faraday Cup, Shield with 3/8-inch Hole	25
6.	Faraday Cup, Long Shield	25
7.	Faraday Cup, Special Shield	25
8.	Mechanical Advantage of Cup Movement	26
9.	Beam-Intensity Cross Sections, Variable-Focus Electrode Voltage	27
10.	Spreading of Originally Parallel Proton Beam Due to Space Charge	28
11.	Ion Trap	29
12.	Beam-Intensity Cross Sections, Space-Charge Effects	30
13.	Spherical Aberration	31
14.	Chromatic Aberration	31
15.	Beam-Intensity Cross Sections, Aberration Effects	32
16.	Total Current vs. Energy, Coulomb Losses	33

LIST OF ILLUSTRATIONS

Figure		Page
1	Block Diagram of Ion Source	11
2	Cross Section of Arc Chamber	13
3	Focusing System of Three Electrodes	15
4	Block Diagram of Gaseous Injection System	18
5	Original Faraday Cup, Shield Hole 3/8 Inch Hole	19
6	Faraday Cup, Zero Shield	19
7	Faraday Cup, Shield Hole	21
8	Mechanical Assembly of Ion Accelerator	23
9	Beam-Injector Cross Sections, Various Three Electrode Systems	27
10	Operating Characteristic Curves, Beam Use vs Space Charge	29
11	Ion Trap	30
12	Beam Injector Cross Sections, Beam-Charge Density	32
13	Spherical Aberration	34
14	Electronic Neutralizer	37
15	Beam Intensity Curve Sections, Aberration Circle	39
16	Total Current vs Energy, Coupled Lobes	41

CHAPTER I

INTRODUCTION

An ion source provides the flow of ions which are the bombarding particles of an accelerator. The kinds of ions that are utilized by present accelerators are protons ($_1H^1$), deuterons ($_1H^2$), and alpha particles ($_2He^4$). Lithium ions have been used infrequently. In some cases, ions of tritium ($_1H^3$) or light helium ($_2He^3$) are desired, but these are generally obtained by nuclear processes rather than from an ion source. Since the Bevatron is designed for the acceleration of protons, this paper will be confined to ion sources that deliver protons.

The original ion source used in the Bevatron was basically the same as that developed by Gow and Foster [1] for the Radiation Laboratory, University of California 32-Mev proton linear accelerator. With only minor modifications this design, shown in Fig. 1, is still in use. The arc chamber used in this source, shown in detail in Fig. 2, is of the type generally known as a Penning or Phillips ion gauge [2] . Such an arc chamber was chosen because it has one of the most simple geometrical forms that will produce a stable discharge. Aside from simplicity, its advantages are low-pressure operation, high efficiency, no filament, and small physical size. Axial extraction of the ions is employed because it is the simplest means of withdrawal. The three focusing electrodes are placed in typical electron-gun fashion, and are referred to throughout this paper as the probe, the focus, and the accelerating electrodes.

Atomic hydrogen gas that is to be ionized in the arc chamber of the source is obtained by passing hydrogen gas through a palladium leak. This atomic gas is immediately introduced into the arc chamber, where a strong electric field is utilized to strike an arc between anode and cathode. An electron released from a cathode, which is made of uncoated aluminum, is accelerated toward the anode. As the entire arc chamber is centered in a coil which provides an axial magnetic field of high intensity, radial motion of the electron is constrained by this

INTRODUCTION

field. The constraint may be such that the electron is accelerated into the anode, coasts through the field-free region within, loses energy through collisions with the gas, and emerges from the other end with somewhat less energy than it gained in its initial acceleration. It is reflected by the electric field, is constrained again by the magnetic field, re-enters the anode, and continues its axial oscillation. During its oscillation it produces several ion pairs, losing energy of the order of 35 volts per pair, and finally it falls below ionization energy and subsequently is taken up by the anode. Since the initial energy of the electron is several hundred volts, it produces approximately ten ions within the anode during its oscillations. These ions are also constrained by the magnetic field so that their principal motion is axial. Eventually, they come to one end of the anode, where they are accelerated into the corresponding cathode. Some of those accelerated into the forward cathode pass through the exit hole and become useful proton beam.

A proton of several hundred volts energy incident on the cathode surface has a finite probability of releasing a secondary electron. Electrons so released will have life cycles as described above. No good data are available on the magnitude of the proton-to-secondary-electron ratio for aluminum oxide, but Gow and Foster [1] estimate that it lies between five and ten. If more ions than this figure are produced by the first electron, the discharge will increase in intensity until limited by other mechanisms.

A fundamental problem within the arc chamber is that of the mean free path for ionization. Let us call it λ_i, and d the mean length of an electron path from cathode to anode. For a single electron emitted by the cathode the probability of ionization is approximately d/λ_i, where d is considerably less than λ_i. If the pressure in the arc chamber were equal to that in the accelerator, λ_i would be equal to several hundred meters. If this were the case, the rate of ionization would be exceedingly low. If we take d equal to ten centimeters and λ_i as 200 meters, we will get approximately one ion for every 2000 electrons. And since the exit hole in the cathode through which ions are drawn is only 0.050 inch in diameter, the rate of removal of ions is generally low. Considering probabilities of production and of extraction, we will

get relatively few useful ions.

To state it simply, the pressure in the injection system and through the Bevatron must be sufficiently low to allow the accelerating ions to travel from the source to the target without colliding with residual neutral atoms. On the other hand, electrons emitted by the cathode must have a high probability of colliding with atomic hydrogen atoms within the arc chamber in order to give a high rate of ionization. These requirements are met by (a) utilizing a high-speed pumping system which permits relatively high pressure within the arc chamber, and (b) forcing the electrons to follow complicated paths before reaching the anode, as described above.

Pulses of current through the arc chamber are provided by a three-kilovolt power supply that is capable of three amperes of current during millisecond pulses, such pulses coming twice per second. Thus pulses of protons, mixed with ionized molecular hydrogen, are emitted from the exit hole in the cathode with the same frequency.

The presence of ionized molecular hydrogen is, of course, undesirable. Such ions are not acceptable for the Bevatron, which is synchronized for the charge and mass of the proton, and they take the place of protons in the ion stream. Several investigators [3] have sought to increase the output of similar sources by introducing impurities that ionize at low voltage, such as mercury vapor. They found that these impurities generally give a manifold increase of the beam current, but magnetic analysis shows that almost all the ions arise from the impurities. Useful current is actually decreased.

The proton-to-molecular-hydrogen ratio can be varied within limits, however, In general, higher arc currents, stronger magnetic fields, and lower arc-chamber pressures give the more favorable ratios. Under good operating conditions with the type of chambers utilized in these experiments, 75 percent protons are obtained, but under normal operating conditions a common figure is 60 percent protons.

The size of the exit hole in the arc chamber is necessarily a compromise. Although the number of protons emitted increases with increase in aperture size, the increase realized is somewhat less than

directly proportional to the area of the aperture [4] . And a larger hole results in higher pressure throughout the subsequent system, which is obviously undesirable, and offers a larger object to the focusing system, which results in a larger image spot. Larger holes also complicate control of the plasma emission surface, such control being accomplished through adjustment of the probe electrode voltage. With no probe voltage, the plasma surface protrudes from the exit hole in tongue fashion. Increasing the probe voltage causes the plasma surface to retreat back into the hole until, under the most favorable emission conditions, the surface is perpendicular to the axis of the source. If the hole is made too large, however, the plasma can no longer be forced back properly by probe voltage, the plasma surface is not perpendicular, and beam current decreases. The exit-hole diameter that has been found to be the best compromise is 0.050 inch.

The focusing action of the three electrodes is shown in Fig. 3. Protons emerging from the exit hole are accelerated to approximately 20 kilovolts by the probe electrode, decelerated to about eight kilovolts in the focus electrode, and accelerated to 45 or 50 kilovolts in the accelerating electrode. With these voltage settings, a real image is obtained approximately one foot beyond the accelerating electrode.

The output beam from the ion source goes into a Cockcroft-Walton column, (refer to Fig. 4), which accelerates the protons to 500 kilovolts. A turning magnet then deflects the beam 20° and sends it into the buncher, a resonator which increases the height of the proton pulse and decreases its width. The beam then enters the linear accelerator to be raised to ten Mev and, finally, is turned 35° by an electrostatic inflector and injected into the Bevatron proper.

Each of the stages subsequent to the ion source constitutes a focusing system, and the combination of these systems is a compound lens of great complexity. It is thus to be expected that the maximum current reading immediately beyond the ion source or at the end of the Cockcroft-Walton column will not necessarily result in the highest current output for the Bevatron. Indeed, the requirements of the Bevatron are unique, and the efficacy of a source can only be determined by trial and error settings while it is pulsing into the Bevatron.

CHAPTER II

FOCAL PROPERTIES OF A TYPICAL ION SOURCE

The purpose of the experimentation herein described was not to improve the design of the arc chamber, whose operation is described in some detail in the previous chapter, but rather to study means of controlling the beam obtained from such a chamber. The source selected for this study is identical to the one employed in the Bevatron with the exception of the diameter of the focusing electrodes, which are two inches in the former and 1-1/4 inches in the latter. Variation in total output with variation of the focusing-electrode voltages was of interest and was investigated, but the main effort was directed toward obtaining beam-intensity patterns that would show the focal properties of the three-electrode system.

1. Operating conditions.

The pressure in the arc chamber during these experiments was 125 ± 25 microns, and the pressure at the end of the accelerating electrode was about 3×10^{-5} millimeters of mercury. Current in the magnet coils surrounding the arc chamber varied from 0.5 to 1.2 amperes, depending upon the setting needed for stable operation, and this resulted in a magnetic field strength within the chamber varying from 500 to 1000 gauss. Voltage across the arc during a pulse was of the order of 300 volts, with the setting of the arc pulser varying from one to two kilovolts as required for stable operation. Arc current varied from one to three amperes, depending upon the requirements of the experiment.

High-current arcs over long periods necessitate frequent replenishment of the oxide layer on the aluminum cathodes. This is done by running the arc on oxygen for a half hour or so. And, from time to time, the aluminum cathodes are found to form compounds, believed to be carbides of aluminum, on their emission surfaces and must be removed and polished. Complications of this sort make settings for a stable arc somewhat variable, but in most cases results obtained were reproducible within ten percent.

2. Measurement techniques.

The first device used for current measurements was a shielded Faraday cup with a 3/8-inch entrance hole (see Fig. 5). It was found that making the cup six volts positive with respect to its shield would decrease current readings by as much as 15 percent. Additional positive bias would decrease current readings still farther, at a decreasing rate, with 90 volts bias resulting in current readings 30 percent below the no-bias figure. Such a fluctuation of current readings showed clearly that electron currents were playing a major role in the readings. Before meaningful beam current readings can be obtained, the magnitude of the electron currents must be known and their effect minimized.

The purpose of positive bias is to draw back secondary electrons formed on the cup and prevent their passing out the entrance hole, being accelerated back through the source, and causing erroneous beam-current readings on the high side. A bias of the order of six volts positive should be sufficient to reclaim all secondaries to the cup, and the decrease in observed current for such a bias is almost assuredly due to this action. The further decrease in current with larger biases indicates that secondaries formed on the lip of the entrance hole were being drawn to the cup and causing erroneous readings on the low side.

In order to provide a long field-free region and minimize the effect of secondary electrons formed at the entrance hole, a device shown in Fig. 6 was constructed. Tests on this device showed that multitudinous secondary electrons were formed on the inside surfaces of the shielding cup when the cup was inclined to the beam. So many of these electrons came into the Faraday cup to be recorded that negative current readings were obtained for all but an axial position of the cup. Clearly this was a much poorer design than before.

To minimize both positive and negative errors in current readings, a device shown in Fig. 7 was developed and has been used for the bulk of the data collected. The field-free region between the two entrance holes makes it unlikely that secondaries formed on the lip of the outer hole will find their way to the cup. A positive bias of six volts on the cup makes it unlikely that secondaries formed on the cup will escape and go back through the source. Readings were found to vary less than

15 percent for the range of biases up to 90 volts.

Small permanent magnets placed around the entrance hole of this device might further reduce errors. Thonemann [5] reports success using a magnetic field of several hundred gauss parallel to the surface of his target cup. In this strong field the secondary electrons, which are relatively slow, are immediately sent back to the cup.

3. Beam-intensity patterns.

The measuring device described above was mounted on the end of a rod (see Fig. 8), which passes through a vacuum seal and provides a means of positioning the cup within the vacuum chamber. The rod can be pushed into the vacuum chamber until the cup lies only two inches from the exit of the accelerating electrode, or pulled out until the cup lies next to the vacuum-chamber wall and is 15 inches from the accelerating electrode. When in the latter position, the exposed end of the rod moves 5.6 inches for each inch of movement of the entrance hole on the cup shield. Thus by plotting positions of the free end of the rod, one obtains quite accurate knowledge of the position of the entrance hole within the chamber. To take advantage of this magnification, all readings for beam intensity patterns were made with the cup at its fully withdrawn position. Total beam currents were obtained by integration of the individual currents throughout the observation plane.

The patterns that are shown as Fig. 9 were obtained by leaving all settings constant while varying the voltage on the focus electrode. There is seen to be a sharp focus at five kilovolts with the pattern flattening and spreading out for voltages above and below this setting. The minimum size of the pattern is of the order of one-half inch in diameter, and for this pattern the central peak carries a current of 0.12 milliampere through an aperture 0.042 inch in diameter.

A peculiar property of these patterns is the definite ring effect that is noticeable for focus-electrode settings of 6.2 and 7.1 kilovolts. Similar rings are observed with a thick lens in conventional optics, but there they are most prominent when the observing plane lies outside the focal plane of the lens. The patterns herein obtained show pronounced rings only when the observing plane lies inside the focal plane

of the lens system. Similar rings were noted at other times when data of this type were recorded. They are even more noteworthy for the virtual-image source, which is described in Chapter IV.

4. Probe electrode length.

It was believed the distance from the probe hole to the focus electrode might be greater than necessary and that a shorter drift distance within the probe might result in a sharper focus. To carry out this experiment, it was first necessary to determine whether displacement of the magnet to the rear would adversely affect the operation of the arc chamber. It was found that moving the magnet back one and one-eight inches decreased the beam current by 25 percent. Runs were also made to see what effect displacement of the magnet has on proton content of the beam. This was done with a magnetic deflecting device which permits separate readings of proton and molecular hydrogen currents. It was found that magnet displacement did not significantly affect the ratio of protons to molecular hydrogen.

A probe 5/8 inch shorter than the usual one was constructed and installed. The arc chamber was moved toward the probe a corresponding distance. The magnet, which lies flush against the back of the source, could not be moved forward, but the effect of this variation of field strength through the arc chamber had been discounted as noted above. Intensity patterns for this arrangement disclosed a decidedly poorer focusing ability for the system, with flat patterns the rule and focus-electrode voltage of little use in sharpening them up.

Lower arc currents were used for additional patterns with the shorter probe. The fact that the focusing ability of the system notably improved with less beam current indicates that the spreading out of the beam in "pancake" fashion is mainly due to space-charge effects.

A shorter probe was decidedly detrimental; it was decided to explore the operation of a longer one. A probe one inch longer than the customary length was installed. Intensity patterns taken with conditions duplicating previous tests with the customary probe indicate that beam current decreases slightly and focusing ability of the system improves somewhat. Neither effect is pronounced enough to establish whether

the longer probe is preferable; the likelihood is that either will serve equally well.

5. Probe-electrode aperture size.

The size of the probe hole that lies over the arc-chamber exit hole has customarily been about 0.1270 inch in diameter. It seemed desirable to determine the gross effects of enlarging and decreasing the size of this hole by 50 percent. A probe with a hole of 0.1890 inch diameter was tested first, and under optimum conditions beam current was down by a factor of eight from that realized with the normal hole. Tests with a probe having a 0.0760-inch hole were equally unrewarding, the total beam current in this case being down by a factor of three. These decreases in beam current are great enough to establish the optimum size probe hole as in the neighborhood of 0.1270 inch.

6. Probe-tip and exit-plate shapes.

The probe has customarily been machined to form a 90° cone with its entrance hole at the apex. The exit plate is customarily a 90° hollow cone. The probe fits concentrically into the exit plate with the tip of the probe spaced about 1/16 inch from the exit hole. Gow and Foster [1] report that less acute cone angles cause an appreciable fraction of the beam to strike the probe.

Tests were made with the exit plate essentially flat and with the conventional 90° probe. No noteworthy alteration in beam-current output or in focal properties of the system was observed. A probe with a hemispherical surface on its end was developed and used with a hemispherically shaped exit plate of slightly larger radius. This design seemed to be as good in all respects as the others, and in addition it gave less trouble through sparking between the probe and exit plate.

CHAPTER III

LOSSES THROUGH SPACE-CHARGE REPULSION, LENS ABERRATION, COULOMB SCATTERING, AND RESIDUAL GAS

The desired product of this focusing system is an image free of distortions. It is further desirable that a minimum attenuation of the beam occur while it is being focused. A perfect image may be obtained only if the extent of the object and image as well as the inclination of the image-forming proton rays are exceedingly small, if the velocity of the protons is uniform, and if the proton concentration at all points of the path is so small that the mutual repulsion of the protons has negligible effect. If these three conditions are not fulfilled geometrical aberrations, chromatic aberrations, and space-charge defects arise, the result of each being to decrease useful beam current. A further obvious source of image imperfections is mechanical misalignment or defective construction of the electrodes an (or) the exit aperture.

1. Space-charge repulsion.

The ability of a focusing system to obtain a sharp focus is dependent in large measure upon the effect of space-charge repulsion on the beam. Space-charge effects as observed for charged particles have no parallel in light rays. A strong concentration of protons at any point has the effect of reducing the potential or decreasing the speed of the individual protons. In a beam of given cross section, this concentration is inversely proportional to the velocity. Thus space charge plays a role primarily in low-velocity, high-current beams. Here it produces a spreading of the beam, resembling the effect of a negative lens (see Fig. 10).

Let us consider two identical charged particles traveling together at the same speed. They exert on each other two different forces; (1) an electrostatic repulsion

$$F_R = \left(\frac{1}{4\ r\epsilon_o}\right)\left(\frac{q}{r}\right)^2 ,$$

and (2) a magnetic attraction, because they correspond to parallel currents

$$F_A = \left(\frac{\mu_o}{4r}\right)\left(\frac{qv}{r}\right)^2 .$$

It may be seen that

$$\frac{F_A}{F_R} = v^2 \mu_o \epsilon_o = \left(\frac{v}{c}\right)^2 .$$

In the case of protons of energy 20 kilovolts, v is only 2×10^6 meters per second, so that F_A/F_R is about 3×10^{-5}, and we see that F_A can be neglected. This would not be the case for electrons of the same energy.

For either electrons or protons the effect of mutual repulsion is far from negligible. For a one-milliampere beam of electrons with an energy of 20 kilovolts, the speed is 8.5×10^7 meters per second and the charge density is 1.2×10^{-11} Coulomb per meter. On the other hand, protons with the same energy have a much lower speed, and their charge density would be 4.5×10^{-10} Coulomb per meter. Thus we see that the space-charge repulsion of a proton beam is much higher than for an electron beam of the same energy, because the charge density is higher and the attractive force is negligible.

A complete treatment of this problem has been made by Fowler and Gibson in "The Production of Intense Beams of Positive Ions." [6] . Their results may be summarized as follows: Consider an initially parallel beam a centimeters in radius; its radius due to space-charge repulsion becomes $2a$, $3a$, $4a$ at distances given by $0.00188A$, $0.00280A$, $0.00358A$, where

$$A = \frac{a U^{3/4} Z^{1/4}}{M^{1/4} I^{1/2}} ,$$

with U expressed in volts and I in amperes; Z is the number of elementary positive charges and M the molecular mass of the ions. Fowler and Gibson state that, for instance, for a proton beam of

20 kilovolts initially 0.375 centimeter in radius, the corresponding distances are 16.8, 24.9, and 31.9 centimeters.

While the above rigorous discussion may well be accurate, Field, Spangenberg, and Helm [7] have shown that positive-ion neutralization of space charge can be attained even at low pressures by means of an "ion trap." This trap (see Fig. 11) consists of suppressor rings at the ends of electrode tubes with a sufficient positive bias to contain positive ions within the electrode. Under these conditions, the investigators report, positive ions are unable to leave the tube, and accumulate in such number that the electron space charge, which would ordinarily depress the potential in the center of the tube, is almost exactly neutralized. Their results show, for instance, that an electron current of 130 milliamperes, traveling 36 centimeters with an energy of 5.7 kilovolts at a pressure of 1/2 micron, suffered no spread in its diameter. Without the ion trap the beam spread to twice its original diameter.

This ion trap is equally applicable to proton currents, obviously, and the principle further raises the question whether the limiting currents, as described by Fowler and Gibson [6], have any meaning, for negative ions within the tubes were not taken into account. Perhaps there are adequate numbers of negative ions within the focusing electrodes of the ion source to neutralize space-charge effects of the beam and lead to very high limiting currents.

To study space-charge repulsion effects in the test source, intensity patterns were obtained for varying beam currents with all electrode voltages constant. Experimental results show that smaller currents definitely result in a sharper pattern (see Fig. 12). Increasing beam current from 6.1 to 8.7 milliamperes, for instance, cut down the peak current at the center of the pattern by a factor of almost two while the diameter of the pattern increased by a factor of one-half. It is thus apparent that, even though the spreading appears to be less than would be predicted by the rigorous treatment, there is considerable loss through space-charge effects in this source. No attempt was made to employ the "ion trap" to lessen these effects.

2. Lens aberration.

The primary contributions to lens aberration for an electrostatic system are from spherical aberration and chromatic aberration. The former, sometimes called aperture defect, is the only geometric aberration which causes unsharpness of the image on the optic axis (refer to Fig. 13). This aberration results in a circle of confusion about every image point, which is proportional in diameter to the cube of the aperture α of the imaging pencil. In magnitude the spherical aberration is the same over the entire image. It is caused by the fact that rays passing through the outer parts of the lens are refracted somewhat more strongly in proportion to the separation from the axis, returning to the axis at a smaller distance from the lens than rays having a smaller inclination to the axis.

Chromatic aberration results from the fact that the deflecting field of a lens acts for a shorter period of time on a proton of greater velocity. Fast protons are thus less affected and focus at a greater distance from the lens than do slow protons. A spread of the image along the axis is produced by this action, as shown by Fig. 14.

The effect of spherical aberration was investigated by obtaining intensity patterns with identical operating conditions and total beam currents for varying beam-input cross section. In the first case (see Fig. 15), the source operated in the usual fashion. In the second case, a 3/32-inch-diameter collimating hole was placed in the probe 3/4 inch from its tip, and this collimator served to reduce the cross section of the beam as it entered the focusing system. Peak current intensity at the center of the pattern was increased by a factor of four by using the collimator. The diameter of the pattern was half as great with the collimator in as with it out. A large portion of the available beam is screened out by such a collimator, however, and the maximum beam current available with it in use is down by a factor of three.

These experimental results indicate that spherical aberration contributes considerably to the spreading of the beam. Since aberration effects are more pronounced at the edges of a lens field, it might be expected that increasing the diameter of the electrodes would improve

The primary restrictions in this observation are electronic speed and low aperture, accuracy and chronometric discretion. The former, accumulation of concrete values, is the only economic alternative which requires precise of the image or the point data. In Fig. 13. This observation examples in a little of location, every image point, accurate proportionality observed to the code or the apparatus a of the timing period. In addition the electrical observation is the third note the method image. It is covered by the bell that pair passing through the upper parts of the lens are relatively economical part strongly in proportion to the resolution (and on basis) relevant to be able at a smaller distance from the lens that they having a reaction position to the axis.

Chromatic observation results from the fact that the deviating field of a lens acts by a shorter extent at that to a portion of greater velocity. Two protons are thus less deviated and image at a greater distance from the lens than an alike protons. A special is the lenses along the axis is produced by this action, as shown in Fig. 14.

The effect of spherical aberration was investigated by measuring in sharply pointed with identical operating conditions and used beam current for varying focal-point-image position. In the first case (see Fig. 15), the source operated in the usual fashion. In the second case, a 1/32-inch diameter collimating hole was placed in the grids. Fig. 16 is a photograph of the pattern produced by a beam of laser by using the collimator. The diameter of the smallest spot that is great with the collimating hole was 0.001 inch. A large portion of the spherical beam is screened by the grid collimator; however, and the resulting beam current available with it does by a factor of three.

These experimental results indicate that spherical aberration includes considerably to the blurring of the beam. Since electrons affected are quite proportional at the object of a lens axis, it might be expected that increasing the diameter of the electrons would improve

the performance of the source by reducing the spreading of the beam. But increasing the diameter of lenses also reduces their focusing strength, and thus the electrode diameter must be a compromise between these two factors.

Chromatic aberration is doubtless present in the over-all problem, but no means was found for independently investigating its effect. Such aberration is very likely present in the above space-charge and spherical-aberration experiments, but we assume that it does not play a prominent role in the effects attributed to them.

3. Coulomb scattering.

The residual gas molecules within the ion source constitute a target material, albeit quite thin, which the protons must pass through. If a proton in the beam should suffer Coulomb scattering off one of these residual molecules, its loss of energy and change of direction would almost assuredly be great enough for it to be eliminated from the useful beam. Thus it is not a question of whether this effect causes losses, as it may be in the case of space-charge effects, but rather of how large such losses are.

Throughout the runs where beam-intensity patterns were recorded with focus-electrode voltage the only variable, it was noted that less total beam current was observed as the focus voltage decreased. The effect was not obvious, however, until the virtual-image ion source was tested. This source operates in an acceleration-acceleration-deceleration manner, the final or accelerating electrode (using previous terminology) being used as the variable or "focusing" electrode. A plot of total beam current versus accelerating-electrode voltage for the virtual-image source showed a much more noteworthy decrease of current with decreasing voltage.

Coulomb scattering of charged particles by target materials is known to vary in such a way that a plot of $1/E^2$ versus log total bombarding current is a straight line, where E is the energy of the bombarding particles. To correlate the loss in beam current as voltage was decreased with losses due to Coulomb scattering, a plot was made with the arguments $1/E^2$ and log total beam current, where E is the energy

of the accelerating electrode. This plot is shown as Fig. 16, and its close approximation to a straight line confirms that the major contributor to the observed losses is Coulomb scattering.

The ratio between total beam current for accelerating-electrode voltages of ten kilovolts and of five kilovolts is a factor of ten. This clearly demonstrates that the losses incurred through long drift distances at low energy are significant.

In the conventional source the losses from Coulomb scattering are not so pronounced as those discussed above because the drift distance at low energy, i.e. the length of the focus electrode, is not great. Improvement in performance of this source is probable, however, if pressure in the focus electrode can be reduced, or voltage increased, or both.

4. Pressure losses.

The losses through increased pressure in the focusing system are similar in magnitude to and inseparable from Coulomb scattering losses. But it was of interest to observe the gross effects of pressure increase in the system, and data were taken for the conventional and for the virtual-image sources.

An increase of pressure from three to six x 10^{-5} mm in the focusing system caused a decrease of beam current of 20 percent for the conventional source operating at its usual settings. A similar increase in pressure with the virtual-image source in operation resulted in the loss of 70 percent of the beam. These results confirm a fact well known, that low pressure is of prime importance.

CHAPTER IV

DESIGN AND TEST OF A VIRTUAL-IMAGE ION SOURCE

Experiments conducted during the autumn of 1954 showed that shortening the length of the Cockcroft-Walton column so as to provide a drift distance between the source and column of about two feet resulted in a significant increase in beam current throughout the system. With this new arrangement the exit hole of the arc chamber, which is the position of the object in the composite lens system, was situated more than three feet from the entrance to the Cockcroft-Walton column. This suggested the possibility of employing a virtual-image ion source, which would eliminate the drift distance introduced between source and column and optically provide a virtual image of the exit hole at the same position, relative to the column, as the actual exit hole had been with the conventional source. Such a source would permit the physical position of the exit hole to be at a minimum distance, about 18 inches, from the Cockcroft-Walton entrance. And if it were possible to duplicate the optical characteristics of the conventional source as seen by the Cockcroft-Walton, considerable gain might be realized as the result of eliminating two feet of drift distance, for drift distance is, of itself, necessarily injurious. These reasons, and the fact that a virtual-image source had never been tried on the Bevatron, prompted the attempt to achieve significant improvement in the useful output of the ion source through use of a virtual-image focusing system.

1. Design.

The arc chamber that had been used for the previous experiments was incorporated into the virtual-image source (see Fig. 1), and the physical dimensions of the housing of the focusing electrodes were retained. Thus the new source could be used interchangeably with the old. The changes made to achieve virtual-image performance were in the length and diameter of the electrodes. A three-inch diameter for the tubes was adopted with the hope that gains from lower pressure and less spherical aberration would be greater than any losses occasioned through

weakening of the lenses. One inch was added to the length of the focus electrode, and the accelerating electrode was retained at its usual length by permitting it to protrude an inch farther from the end of the source than before. The probe length was maintained, but the shape of the probe tip and exit plate were hemispherical instead of 90° cones.

To achieve a virtual image, the electrodes are energized to provide an acceleration-acceleration-deceleration action on the protons. Through approximation calculations on the focusing system, it was predicted that, with 20 kilovolts on the probe electrode and 40 kilovolts on the focus electrode, parallel rays would be obtained for an accelerating electrode voltage of about 12 kilovolts. At some higher voltage, something less than 25 kilovolts, the calculations indicated that a virtual image would be achieved about two feet behind the exit hole. With the power supplies that were to be employed, however, adequate latitude of settings was available to insure optimum placement of the virtual image.

2. Test-stand data.

A series of runs was made with probe voltage set at 14 kilovolts and focus voltage at 40 kilovolts. Although a crossover focus was expected with about eight kilovolts on the accelerating electrode, total beam current was so diminished by Coulomb scattering in this low-energy region that the setting for best crossover was effectively masked and total beam currents were deceptively low. If measurements could have been made within the accelerating electrode rather than at a distance two feet beyond, more indicative patterns and higher currents would undoubtedly have been achieved.

Settings of ten kilovolts and slightly above on the accelerating electrode gave much higher total currents, as would be expected with less scattering, and the patterns were spreading out and flattening in a manner indicative of parallel rays, which would be expected with these settings.

No ready means was available on the test stand for determining positions of a virtual image, and further information on the source could only be achieved by operating it with the Bevatron.

3. Bevatron runs.

Before new power supplies for use with the virtual-image source were

available, a breakdown of the source in the Bevatron necessitated the installation of the virtual source. It was operated at this time with acceleration-deceleration-acceleration settings, and the best results were obtained when voltages were such as to give a real image. The best performance available with this arrangement showed the current at the end of the Cockcroft-Walton to be comparable with that obtained with the usual source, but total beam out of the linear accelerator was down by a factor or two or three. Therefore, the usual source was replaced in the Bevatron when it was again operative.

Later tests with the virtual-image source operating in its designed fashion--probe voltage 18.5 kilovolts and focus voltage 48 kilovolts--showed a definite maximum current through the Cockcroft-Walton with accelerating voltage at eight kilovolts, a minimum point at 13 kilovolts, and a higher maximum with accelerating voltage at 19 kilovolts. Since from test information a crossover was expected at about 8 kilovolts, this indicates that the first maximum was the crossover or real-image condition, the minimum a case where the rays were essentially parallel, and the larger maximum the desired virtual-image operation. Maximum current through the Cockcroft-Walton with the accelerating voltage in the neighborhood of 19 kilovolts was nine milliamperes, which is somewhat less than the 12 milliamperes obtained under good conditions with the usual source at this position. The maximum available current at the input to the linear accelerator was 2.2 milliamperes, which compares even less favorably with the 6.0 milliamperes that can be obtained with the usual source. Current measurements at the exit of the linear accelerator were ridiculously low, however. Whereas the conventional source may register 300 microamperes at this point, the virtual image source could produce only eight or ten microamperes, a factor of 30 down. The new source was clearly not an improvement.

Reasons why the virtual-image source did not get more current through the system are obscure, just as the focusing characteristics of the injection system are, but indications are that the beam was too diffuse, certainly in size and probably also in energy, for it to be accelerated effectively on through the injection system. Smaller tubes

or other changes might improve performance somewhat, but it is quite likely the system prefers a real-image source to any virtual-image source that might be designed.

BIBLIOGRAPHY

1. Gow, J.D. and Foster, J.S., Jr. — A HIGH-INTENSITY PULSED ION SOURCE, The Review of Scientific Instruments, Vol. 24, No. 8, pp 606-610, August 1953

2. Penning, F.M. — Physica 4, 71 (1937)

3. Hoyaux, M. and Dujardin, I. — COMPARATIVE SURVEY OF ION GUNS, Nucleonics Research Laboratories, Ateliers de Constructions Electriques de Charleroi, Belgium

4. Pierce, J.R. — THEORY AND DESIGN OF ELECTRON BEAMS, D. Van Nostrand Company, 1949

5. Thonemann, P.C. — Nature 158, 61 (1946)

6. Fowler, R.D. and Gibson, G.E. — Phys. Rev. 46, 1075 (1934)

7. Field, L.M. Spangenberg, K. and Helm, R. — CONTROL OF ELECTRON BEAM DISPERSION AT HIGH VACUUM BY IONS, Elec. Comm. 24, No. 1, pp 108-121, March 1947

8. Zworykin, V.K. Morton, G.A. Ramberg, E.G. Hillier, J. and Vance, A.W. — ELECTRON OPTICS AND THE ELECTRON MICROSCOPE, John Wiley and Sons, Inc., 1948

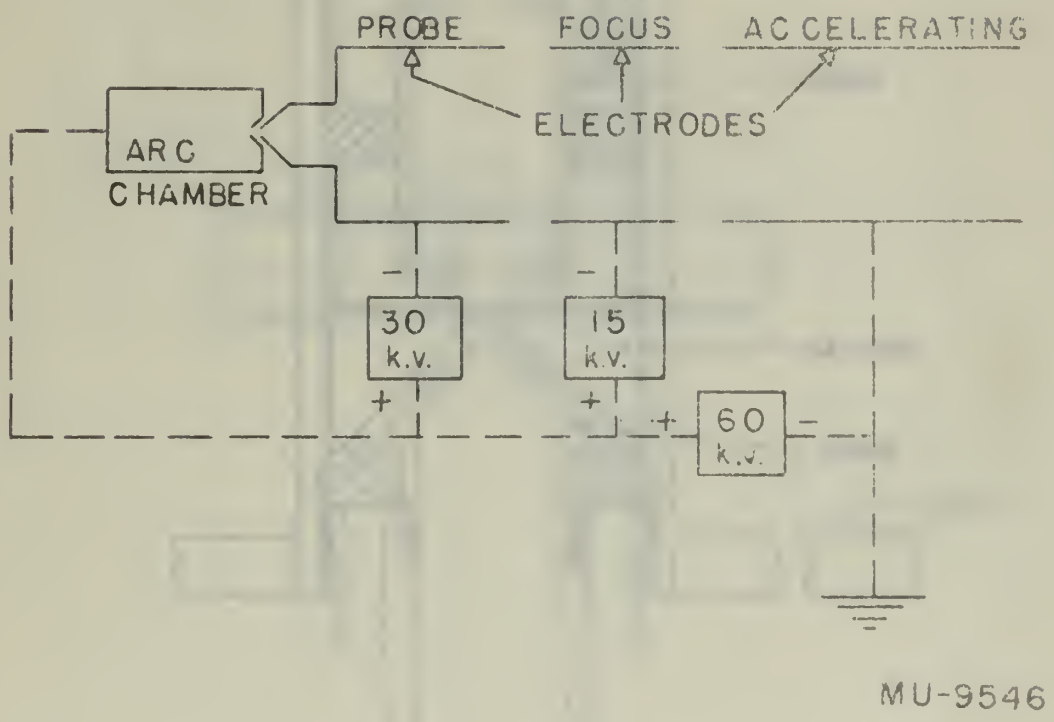

Fig. 1 Block Diagram of Ion Source.
Diameter for Electrode Tubes, 2 in.;
Lengths of Electrodes:
probe, 2 in.;
focus, 2.5 in.;
accelerating, 4 in.

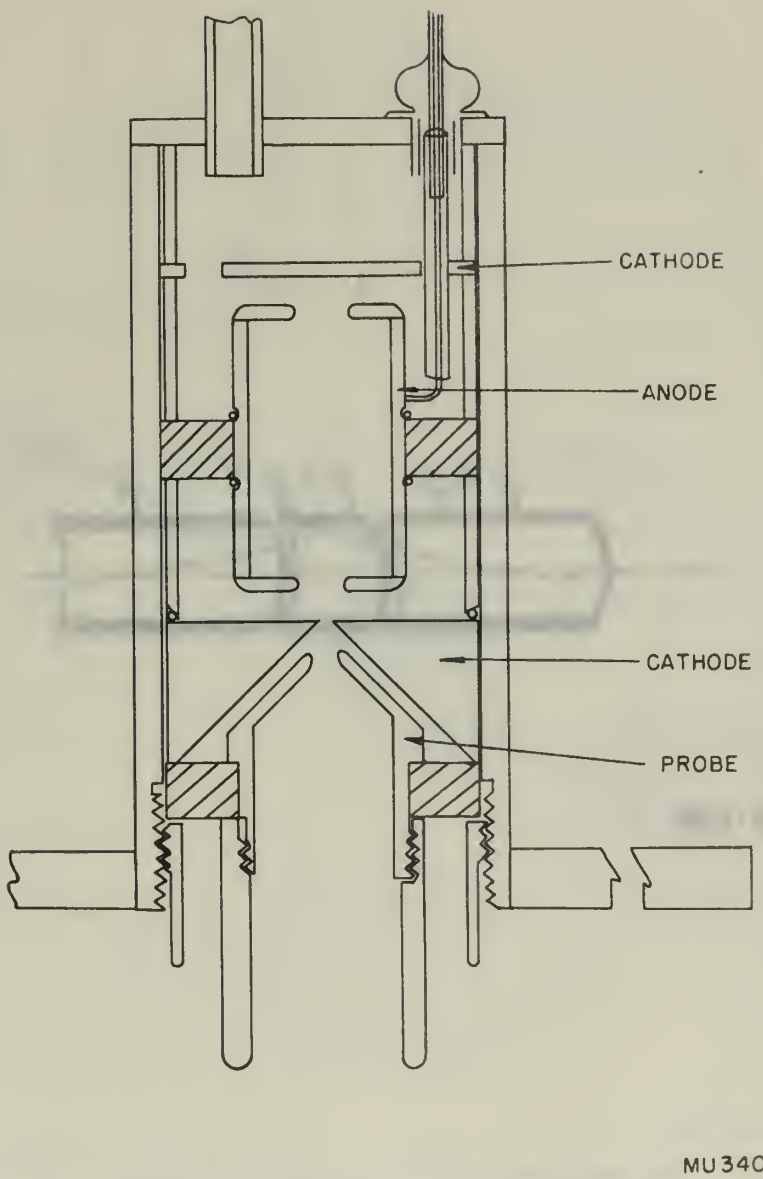

Fig. 2 Cross Section of Arc Chamber

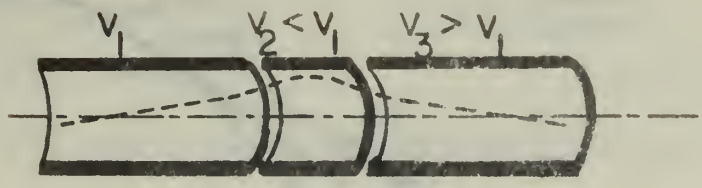

MU-9547

Fig. 3 Focusing Action of Three Electrodes

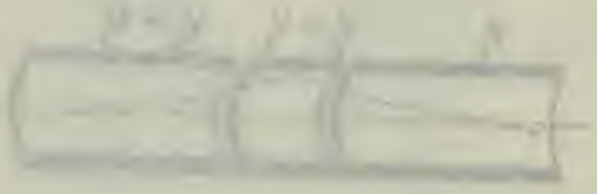

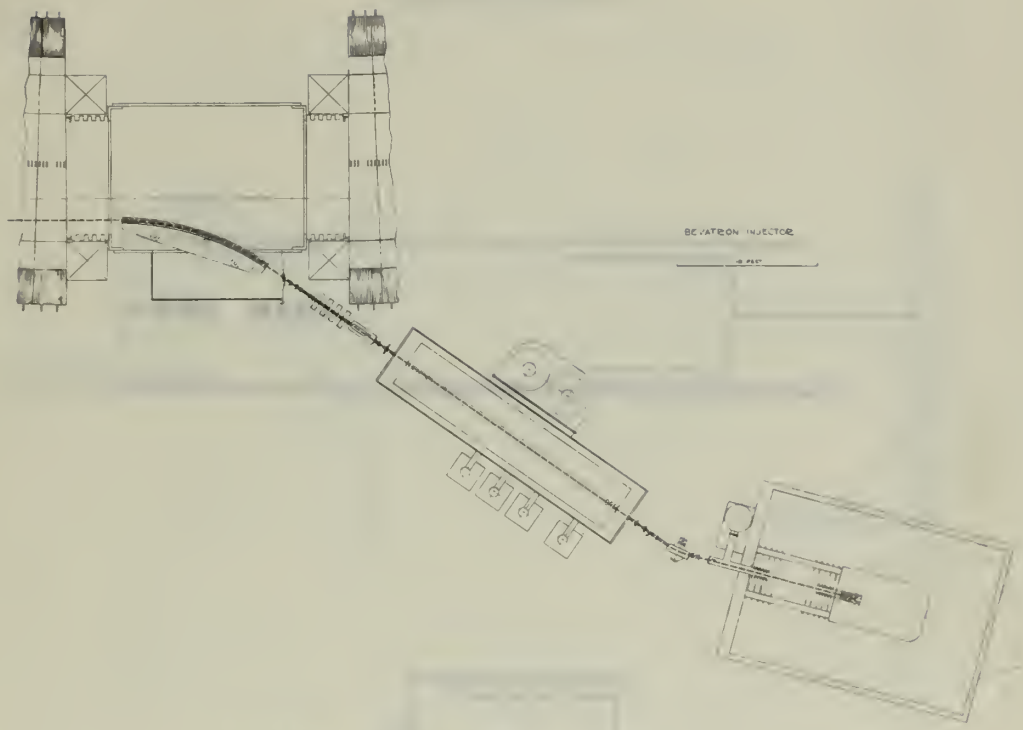

Fig. 4 Block Diagram of Bevatron Injection System

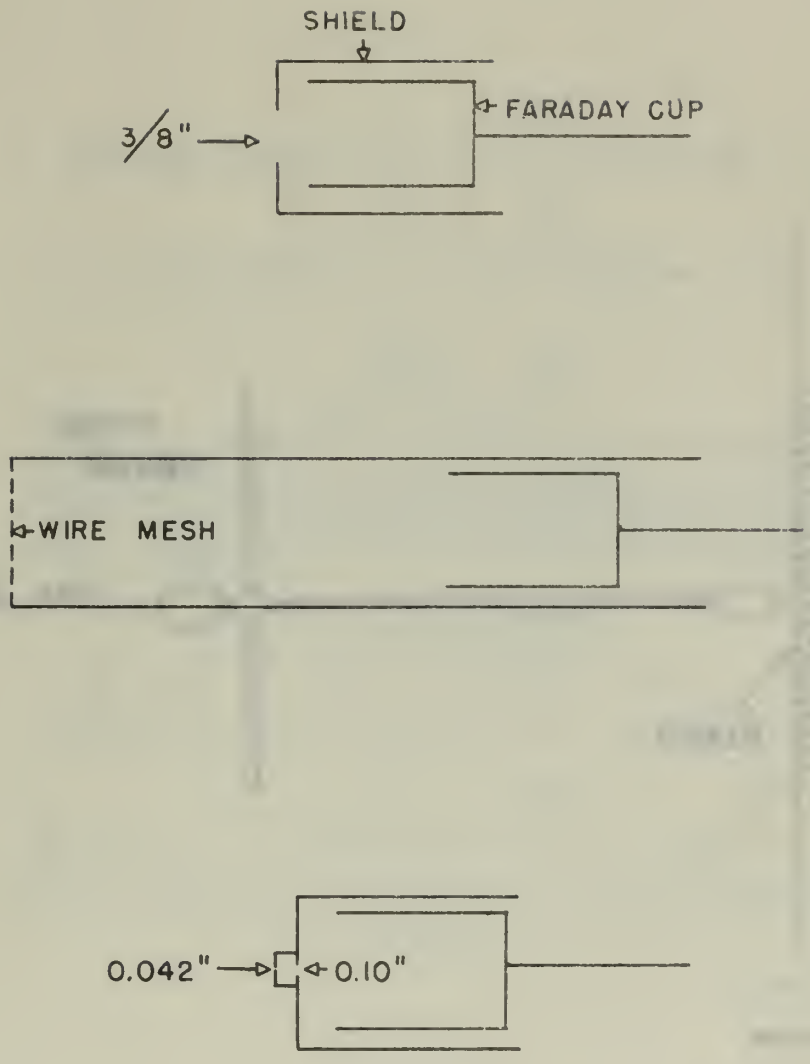

Fig. 5 Original Faraday Cup, Shield with 3/8-inch Hole

Fig. 6 Faraday Cup, Long Shield

Fig. 7 Faraday Cup, Special Shield

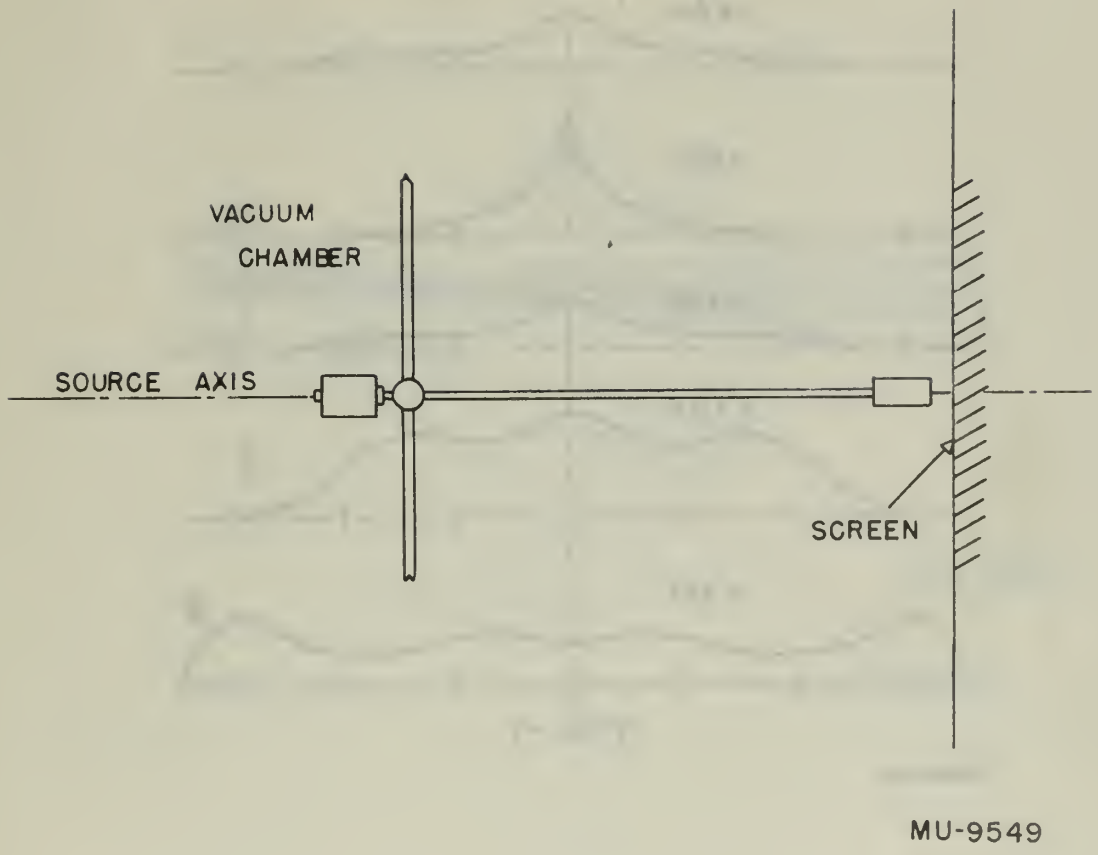

Fig. 8 Mechanical Advantage of Cup Movement

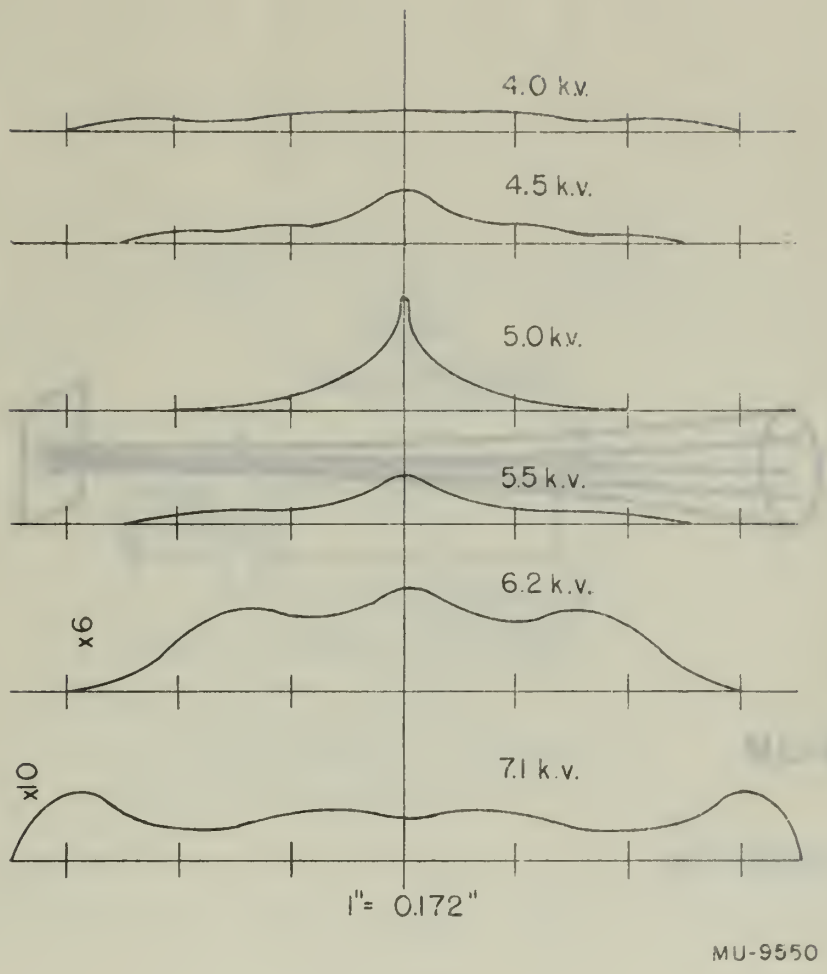

Fig. 9 Beam-Intensity Cross Sections, Variable-Focus Electrode Voltage

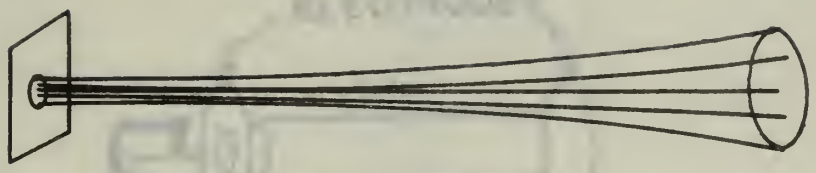

MU-9551

Fig. 10 Spreading of Originally Parallel Proton Beam Due to Space Charge

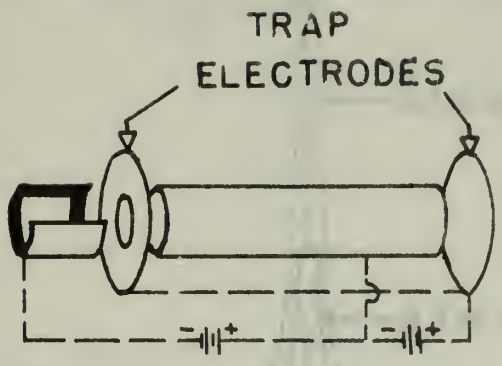

MU-9552

Fig. 11 Ion Trap

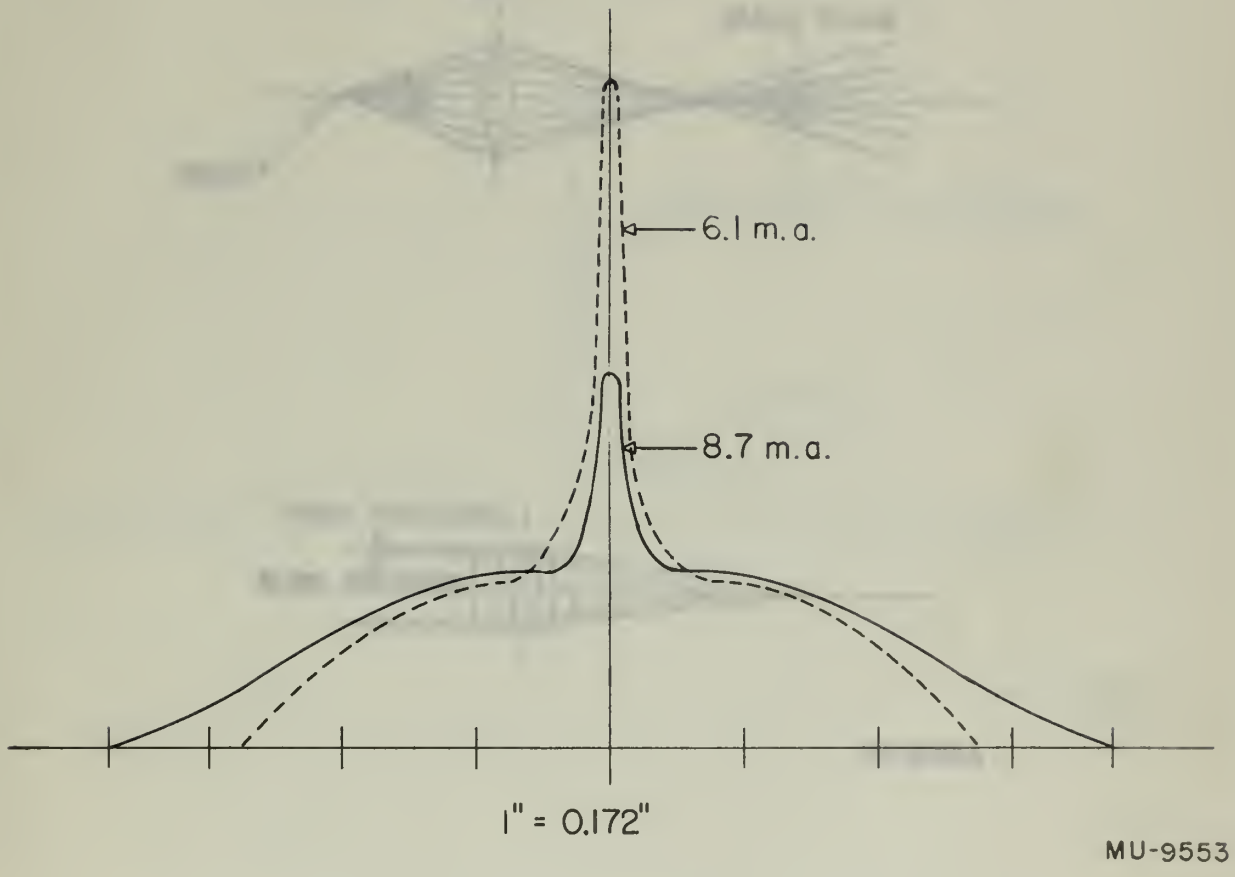

Fig. 12 Beam-Intensity Cross Sections, Space-Charge Effects

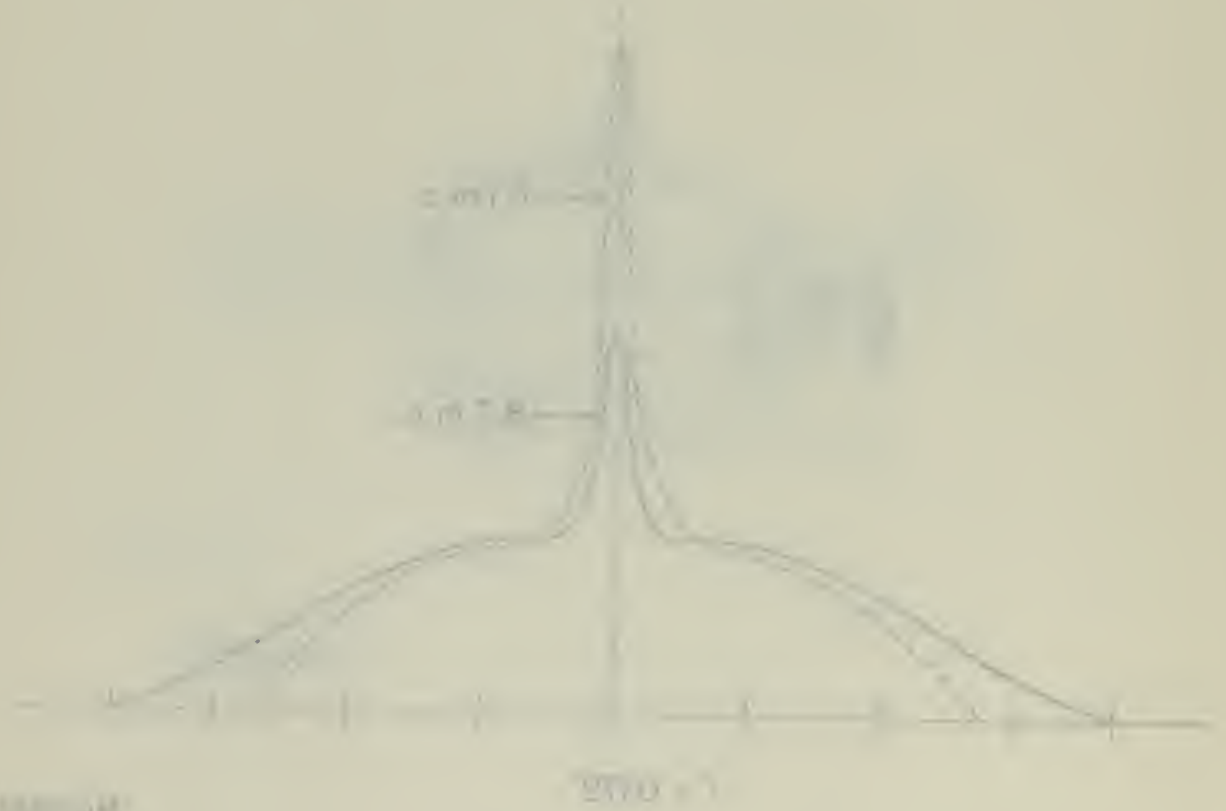

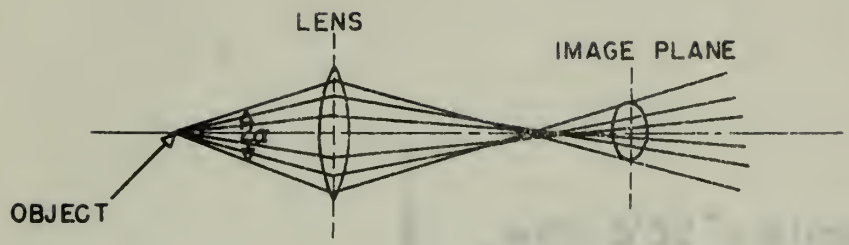

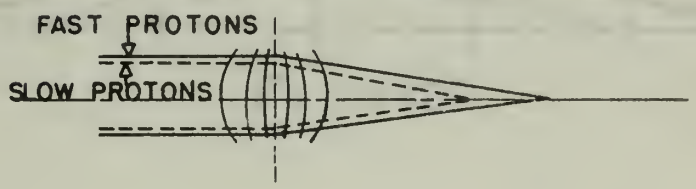

MU-9554

Fig. 13 Spherical Aberration

Fig. 14 Chromatic Aberration

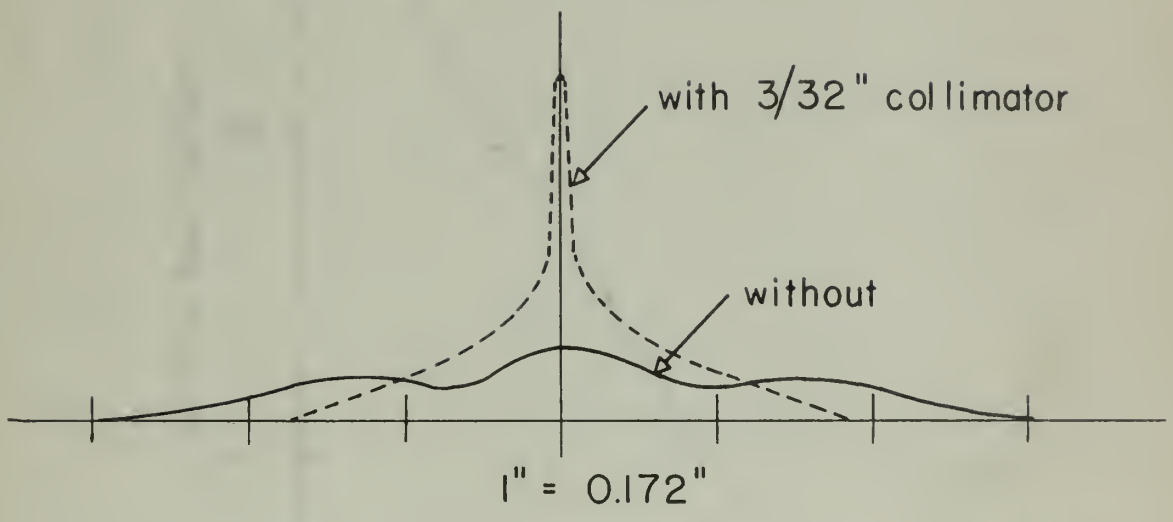

Fig. 15 Beam-Intensity Cross Sections, Aberration Effects

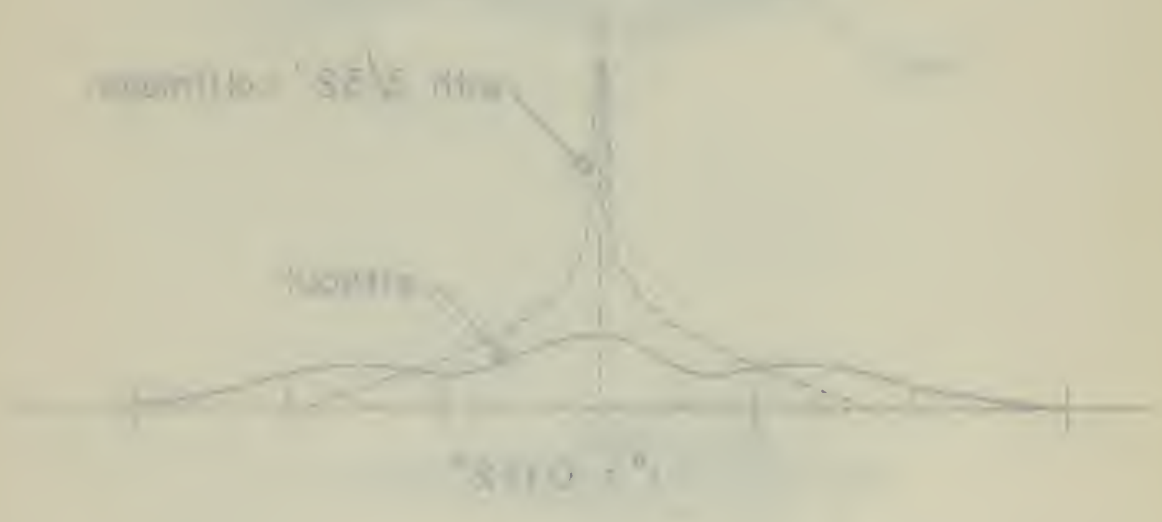

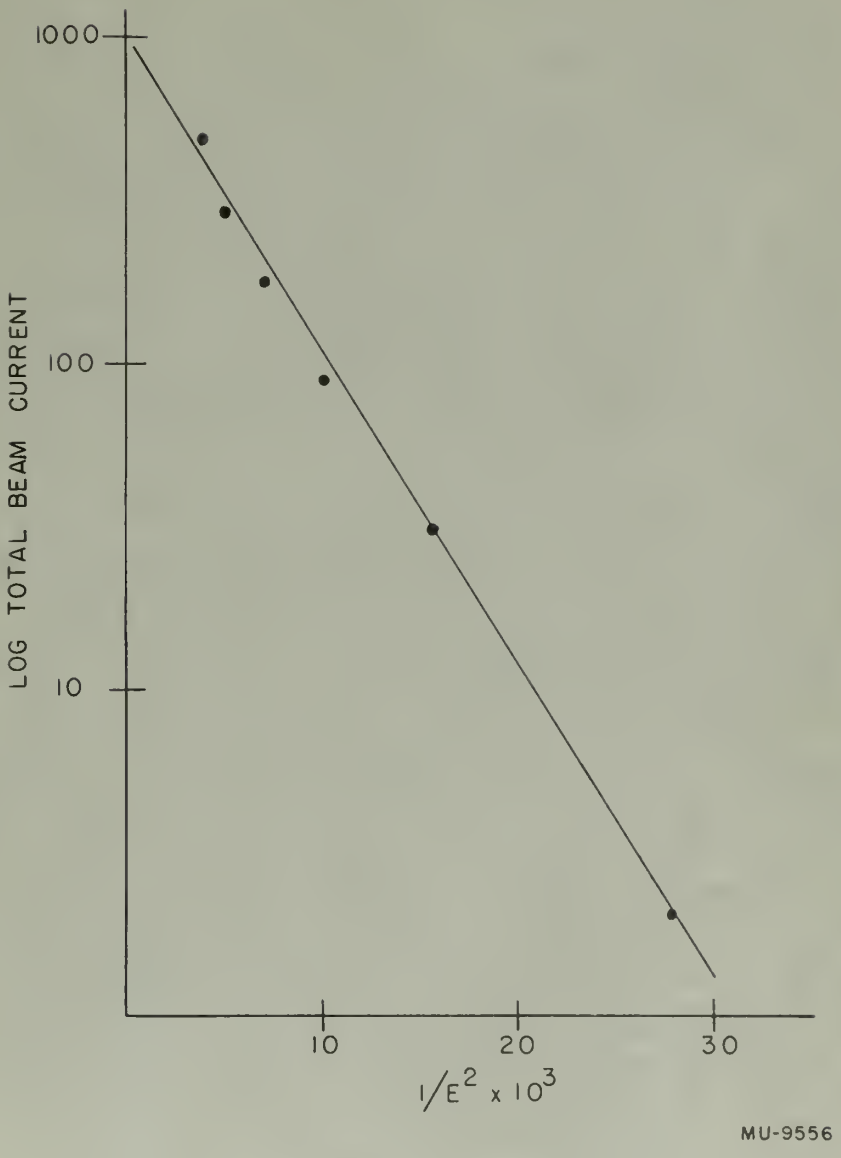

Fig. 16 Total Current Versus Energy, Coulomb Losses
(E is energy of Accelerating Electrode)

JL 1956 INTERLIB
Naval Research Lab

28473

Thesis
S765 Stone
Experiments on improving the efficiency of the bevatron ion source.
JL 1956 INTERLIB

28473

Thesis
S765 Stone
Experiments on improving the efficiency of the bevatron ion source.

thesS765
Experiments on improving the efficiency
3 2768 002 02042 2
DUDLEY KNOX LIBRARY